Pressure-dependent phonon properties of $La_{0.7}Sr_{0.3}MnO_3$

Mina Talati[1] and Prafulla K. Jha[1,*]
[1]*Computational Condensed Matter Physics–CCMP Laboratory, Department of Physics, Faculty of Science, The Maharaja Sayajirao University of Baroda, Vadodara-390 002, India*
(Received 19 April 2006; revised manuscript received 12 June 2006; published 12 October 2006)

In this work, we present the calculated results on the pressure dependent phonon properties of rhombohedral ($R\bar{3}c$) $La_{0.7}Sr_{0.3}MnO_3$ manganite by using a lattice dynamical model theory. The effect of internal pressure determined by the average *A*-site atomic radius is also investigated and compared with the effect of applied pressure. The computed zone center phonon frequencies at ambient pressure agree fairly well with the experimental results and the modes related to the octahedral distortion exhibit hardening with the increase in pressure. The Raman active A_{1g} mode is most sensitive to pressure with a slope of 1.0 cm^{-1}/GPa and shows unusual couple of slope change. Both internal and external pressures harden the A_{1g} phonon mode and reduce the electron-phonon interactions. Change in the frequency of the Raman active E_g modes with frequency is also observed. Different effect is observed for the low and high average *A*-site atomic radius. The phonon dispersion curves in high symmetry directions of the Brillouin zone and phonon density of states are also calculated. The pronounced shift of the peak positions in phonon DOS is observed with the increase in pressure. The analysis of the reduction of the high frequency phonon peak width and effective mode-Grüneisen parameter allows us to draw a conclusion for the decrease in lattice distortion and to some extent Jahn-Teller (JT) distortion, a signature of rhombohedral structure for the manganites. The role of pressure on the lattice specific heat is also discussed.

DOI: 10.1103/PhysRevB.74.134406 PACS number(s): 75.47.Gk, 63.20.Dj, 78.30.−j, 71.15.Pd

I. INTRODUCTION

During the last decade $R_{1-x}A_xMnO_3$ (R=rare earth La, Pr, Nd, Dy; A=alkaline earth ions Sr, Ca, Ba, Pb) manganites have attracted great attention due to their interesting physical properties that makes these systems a promising candidate for the applications as magnetic sensors. The phase diagram of these compounds is rich and complex and many variables such as pressures,[1] temperature,[2,3] magnetic field,[2,4] and *A*-site average ionic radius (chemical pressure) (Ref. 5) determine a wide range of ground states in these systems. Since the physical properties of these states are often sensitive to even a small change in intrinsic and external conditions, there appears to be a number of colossal effects. The colossal magnetoresistance (CMR) effect in these perovskite manganites is one of the best known examples of such an effect.[6] It is observed that the application of a magnetic field induces a transition from a paramagnetic insulating (PI) to a ferromagnetic metallic (FM) phase. The large difference between the resistivity of these two phases lies at the heart of the CMR effect, which can be qualitatively explained by the double exchange (DE) model, first proposed by Zener.[7] But the DE model could not predict measured resistivity quantitatively and a large difference is observed in predicted and measured values. Millis *et al.*[8] argued that the DE alone could not explain the resistivity in these systems and the Jahn-Teller (JT) type lattice distortions of the MnO_6 octahedra should be considered owing to JT distortion. This JT distortion results into the splitting of Mn^{+3} e_g orbital and therefore the energy of the occupied orbital reduces and localizes the states.

In the cubic perovskite ABO_3, due to the radius mismatch of the *A*- and *B*-site atoms, structural distortion is induced. The chemical substitution (doping elements and concentrations "*x*") at *A*-site changes the number of electrons in 3*d* band of Mn, lattice parameters, Mn-O bond length, and Mn-O-Mn bond angle.[9–15] The changes in the doping levels also result in changes in the MnO_6 octahedra and therefore the local distortion is affected. The similar effects can also be achieved by the externally applied hydrostatic pressure. The application of pressure also results in the stabilization of rhombohedral phase of $La_{1-x}Sr_xMnO_3$ (x=0.12–0.18) (Refs. 16 and 17) and $La_{0.8}Ba_{0.2}MnO_3$ (Ref. 18) systems. The application of pressure reduces the lattice constants, increases the Mn-O-Mn bond angles and the unit cell becomes more cubic, and reduces the local distortion of the MnO_6 octahedra and electron-phonon coupling.[19–21] In addition, an increase in T_C is observed as the pressure is increased.[1,21] It is an established fact that the JT distortion plays an important role and hence influences many properties in the manganites. The application of pressure both chemical and external reduces the volume around the *A* ion in the cage of MnO_6 octahedra which results into the symmetrization of the surrounding structure and reduction in JT distortion.[20–22] The coherent and incoherent distortions affected by the high pressure and doping are abruptly reduced when crossing into the ferromagnetic (FM) phase.[23] The electron-phonon (el-ph) interaction is affected by the pressure through the modification of the frequency of the octahedral bending and stretching modes.[24–27]

In recent times, there have been some speculations that for pressures above 2 GPa, the behavior of manganites may be different from that observed in the low-pressure measurements.[28,29] However, Hwang *et al.*[1] found that the effect of pressure could be mapped onto the average radius of the *A*-site atoms with a conversion factor of 3.75×10^{-3} Å/GPa in the pressure range below ~2 GPa. The Raman scattering study of orthorhombic $La_{0.75}Sr_{0.25}MnO_3$ by Congeduti *et al.*[20] showed that the pressure above 7.5 GPa in-

duces a new phase other than the predicted metallic phase. The lattice compression due to the application of pressure results in abrupt change in phonon frequency and strong phonon broadening suggesting increase in electron-phonon interaction. A long-range static/dynamic Jahn-Teller distortion and more distorted MnO_6 octahedra are observed by Meneghini *et al.*[30]

To the best of our knowledge, the high pressure effects on the CMR and its related properties including phonon properties of the optimally doped manganites with the rhombohedral crystal structure of $(R\bar{3}c)$ symmetry are not studied so far. The present study reports the results on the complete phonon properties of rhombohedral $La_{0.7}Sr_{0.3}MnO_3$ under high pressure by using a lattice dynamical model theory under the framework of shell model. The super-exchange interaction between the localized spins is neglected in the present calculation as this is beyond the scope of the present model calculation. The rhombohedral $La_{0.7}Sr_{0.3}MnO_3$ (LSMO) compound exhibits the metallic-like temperature behavior of resistivity and transforms to the ferromagnetic (FM) state at $T_C \sim 370$ K.[31] The $dT_C/dP \approx 5$ K GPa^{-1} for LSMO (Ref. 32) is much smaller in comparison to that obtained in the same pressure range for the other manganites with a close chemical content but in the orthorhombic phase.[33,34] The present study also reports the results on the investigation of the effect of A-site average atomic radius ($\langle r_A \rangle$) on some of the selected phonon modes and phonon spectra. The effect of two different kinds of pressure is also correlated. To see the effect of ($\langle r_A \rangle$), Ba and Pb doped $LaMnO_3$ systems are selected with Sr doped $LaMnO_3$ as reference system. It will be seen in what follows that the effect of these two pressures is different and there is a clear difference in the phonon properties for low and high $\langle r_A \rangle$. Section II describes the brief theoretical methodology for calculating the lattice vibrations. Section III contains the results and discussion followed by the main conclusion in Sec. IV.

II. THEORETICAL METHODOLOGY

In order to calculate the phonon properties of the considered manganites, interatomic potential in the form of a Buckingham potential is used. It has been shown to perform sufficiently well and it is widely used for modeling various oxides. This potential takes the form

$$U_{ij}(r_{ij}) = \frac{Z_i Z_j e^2}{r_{ij}} + b_{ij} \exp\left(-\frac{r_{ij}}{\rho_{ij}}\right), \quad (1)$$

where the first and second term represent the Coulomb potential and Born-Mayer repulsion energies, respectively. Here, r_{ij} is the interatomic distance between ith and jth atoms, Z_i and Z_j are the effective charges of the respective atoms, b_{ij} and ρ_{ij} are the short-range potential parameters for each pair of atoms usually found by fitting to experimental data. For the potentials described, O-O short-range interactions were chosen from Ref. 35, which was successfully used for the modeling of several oxides.[36,37] The electronic polarization of the lattice is included by the shell model where in, an ion is represented by a massless shell of charge Y and a core of charge X which are coupled by a harmonic spring constant K. To calculate the phonon properties the software LADY for lattice dynamical simulation is used.[38] Only the oxygen ions are considered to be polarizable. This model has been quite successfully used in recent times by us.[39,40] We use the same set of model parameters to determine the phonon properties of $La_{0.7}Sr_{0.3}MnO_3$ at all considered pressures but a variation of 3 to 5 % in the case of A/A'-O short-range interactions for Ba and Pb doped systems are allowed. It is ensured that the parameters yield stable structure. The parameters so obtained are listed in Table I.

TABLE I. Input parameters for rhombohedral $La_{0.7}Sr_{0.3}MnO_3$ at 0, 2.2, 5.0, and 7.5 GPa.

Interactions	b (eV)	ρ (Å)
La/Sr-O	1500.0	3.2615
La/Ba-O	1555.0	3.3582
La/Pb	1575.0	3.4237
Mn-O	3030.0	2.9815
O-O	2100.0	2.1978
	Shell model[a]	
Ion	Y (e)	K (eV Å^2)
O^{2-}	−2.86902	74.92

[a]Y and K refer to the shell charge and harmonic spring constant, respectively.

III. RESULTS AND DISCUSSION

The rhombohedral $La_{0.7}Sr_{0.3}MnO_3$ compound has the symmetry of the space group $(R\bar{3}c)$ (D^6_{3d}), which can be generated by the rotation of the adjacent MnO_6 octahedra in opposite directions about the cubic [111] directions. Thus, at zone center following irreducible modes result for the $La_{0.7}Sr_{0.3}MnO_3$ in $R\bar{3}c$ structure

$$\Gamma(D^6_{3d}) = 2A_{1u} + 3A_{2g} + A_{1g} + 4A_{2u} + 4E_g + 6E_u, \quad (2)$$

where the $A_{1g}+4E_g$ are Raman active, the $3A_{2u}+5E_u$ are infrared (IR) active, and the remaining $2A_{1u}+3A_{2g}$ modes are silent modes. La atoms participate in four Γ-point (zone center) phonon modes $(A_{2g}+A_{2u}+E_g+E_u)$. While Mn atoms contribute to four $(A_{1u}+A_{2u}+2E_u)$ Γ-point phonon modes, O atoms take part in twelve $(A_{1g}+A_{1u}+A_{2g}+2A_{2u}+3E_g+3E_u)$ Γ-point phonon modes in the rhombohedral lattice. The structure parameters of $La_{0.7}Sr_{0.3}MnO_3$ at selected pressures and ambient temperature for the calculation of phonon properties in the present study are used from Ref. 19. Since the main aim of the present study is to see the effect of pressure on the phonon properties of $La_{0.7}Sr_{0.3}MnO_3$ and find the most affected phonon modes with the application of pressure and therefore responsible for any unusual behavior particularly related to JT distortion and MnO_6 octahedra. For this reason, present study reports the zone-center phonon frequencies, phonon dispersion curves, phonon density of states, and thermal properties of LSMO at pressure up to

TABLE II. The zone center phonon frequencies for rhombohedral $La_{0.7}Sr_{0.3}MnO_3$ at 0, 2.2, 5.0, and 7.5 GPa. All frequencies are in cm^{-1}.

	Phonon frequencies (cm^{-1})				
Modes	0 GPa	2.2 GPa	5.0 GPa	7.5 GPa	Experimental
A_{1g}	210.78	211.44	214.62	215.05	199[a]
					180[b]
					230[c]
A_{2g}	344.14	346.84	350.38	353.26	
	478.49	486.24	495.37	503.87	
	538.04	546.48	556.20	565.46	
E_g	29.08	29.34	29.88	30.14	42[a]
	174.25	176.32	179.84	182.02	
	408.72	414.44	421.66	427.86	420[c]
	447.57	454.96	463.36	471.50	
A_{1u}	175.61	176.38	179.26	179.89	
	550.17	554.47	560.18	564.78	
A_{2u}	67.31	67.94	69.26	69.90	
	561.51	570.34	580.67	590.36	641,[d] 580,[e] 576[f]
	648.22	653.29	659.99	665.41	
E_u	43.77	44.17	45.00	45.40	
	72.50	73.53	75.13	76.25	
	113.07	114.45	116.79	118.25	
	180.36	182.74	186.50	189.05	
	416.91	423.04	430.64	437.32	

[a]Raman data at 10 K (Ref. 41).
[b]Raman data at 300 K for $La_{0.67}Sr_{0.33}MnO_3$ (Ref. 42).
[c]Raman data at 30 K for $La_{0.8}Sr_{0.2}MnO_3$ (Ref. 43).
[d]Calculated and experimental IR data at 405 K respectively (Ref. 44).
[e]Calculated and experimental IR data at 405 K respectively (Ref. 44).
[f]Inelastic neutron scattering data (Ref. 45).

7.5 GPa. The computed zone center phonon frequencies for ambient and high pressures have been presented in Table II. They are seen to match reasonably well with the available data.[41–45] Since the A_{1g} and E_g modes are directly related with the MnO_6 octahedra and hence the appearance of JT distortion in these compounds,[23] the discussion on the effect of pressure is limited to these phonon modes only. The A_{1g} mode is due to the rotation of MnO_6 octahedra around the hexagonal *c axis*, while the E_g modes are due to the bending of MnO_6 octahedra.[45] The Raman active A_g mode corresponding to an in-phase rotation of the MnO_6 octahedra around the *b axis* in lower symmetry (distorted) orthorhombic structure of these compounds is closely related to the A_{1g} mode in higher symmetry rhombohedral $La_{0.7}Sr_{0.3}MnO_3$ and found to be the most sensitive to the kind and value of the dopant.[23] Figure 1 presents pressure variation of some selected zone center phonon modes. It is seen from this figure that the frequencies of both IR and Raman modes involving the vibrations of La atom do not show any change with pressure while the modes (E_g and A_{2u}) involving oxygen atom vibrations (high frequency) and related to the MnO_6 octahedra show linear pressure induced hardening. The low frequency phonons are ascribed to pure *A*-atom vibrations, which actually do not depend on the octahedral distortion. The pressure variation of the Raman active A_{1g} mode shows an unusual couple of slope changes in the considered pressure range, which may be ascribed to some abrupt change of

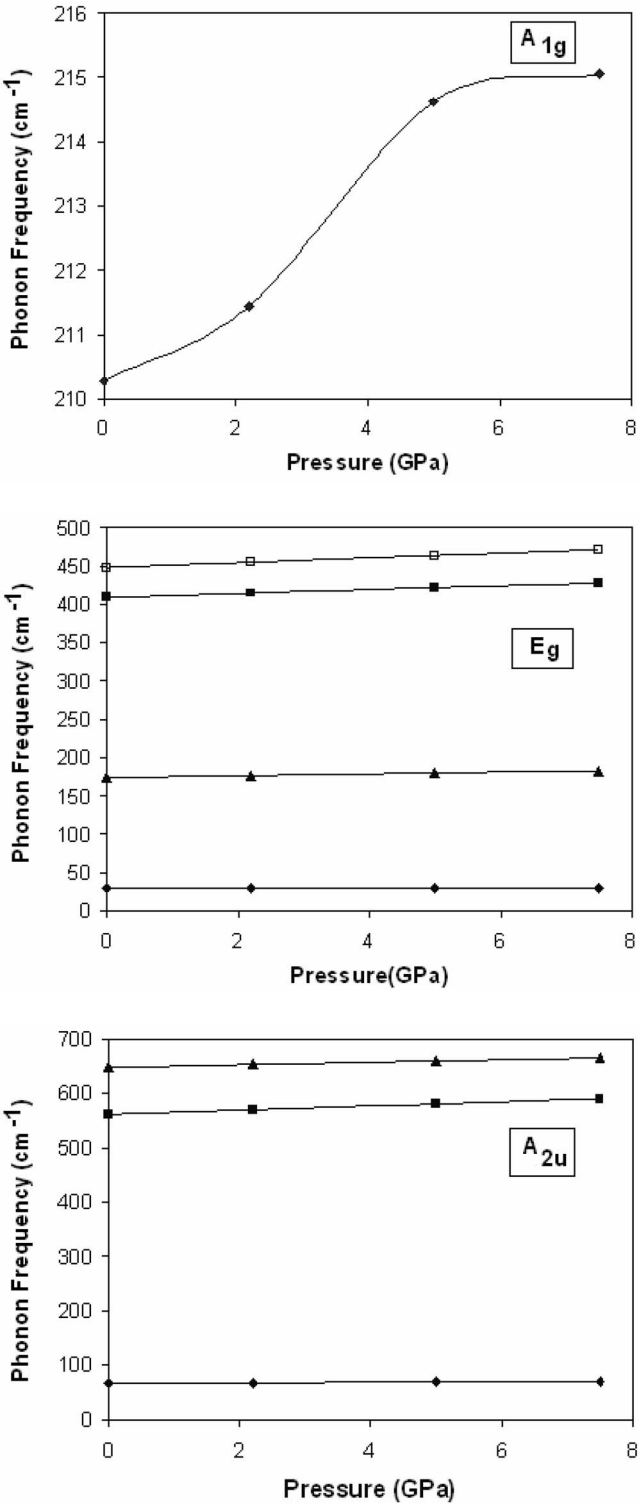

FIG. 1. Pressure variation of some zone center phonon modes.

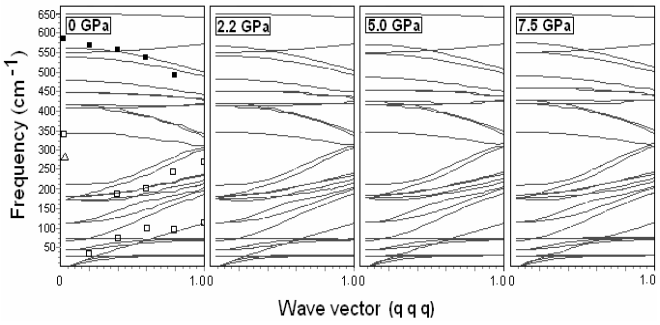

FIG. 2. Pressure variation of phonon dispersion curves (PDC) of $La_{0.7}Sr_{0.3}MnO_3$. Open and filled symbols represent INS data at ambient pressure (Ref. 45).

the JT distortion. The $d\omega/dP$ is not too large for this mode but it saturates for pressures above 5.0 GPa. The pressure behavior of the stretching and rotational modes (A_{2u} and E_g, respectively)[43] with $d\omega/dP$ of about 4 cm^{-1}/GPa suggests that the Mn-O-Mn angle is close to the ideal 180° value of the cubic structure and therefore the system would be of more metallic character.[19] It is known that the electron-phonon coupling affects the transport properties of manganites and it is strong for insulating phase and weak in metallic phase. Therefore, the present observations prompted us to conclude qualitatively that the pressure causes a decrease of electron-phonon coupling as system transforms to metallic state from its original insulating state. Also, these frequency shifts indicate that the Mn-O-Mn bond angle and the Mn-O distance changes meet the metal-insulator transition. The rotational frequency of MnO_6 octahedra is not changing fast indicating that the octahedra are not severely distorted by the application of pressure. Therefore, it can be concluded that the hardening of phonon frequencies is consistent with the increase in T_C with pressure.[19] The similar increase in the stretching mode is observed earlier for $La_{0.75}Ca_{0.25}MnO_3$ (Refs. 20 and 21). The concentration and temperature dependent Raman investigation performed by Bjornsson *et al.*[43] shows the appearance of new phonon modes at about 230 cm^{-1} and 420 cm^{-1} in rhombohedral phase of $La_{1-x}Sr_xMnO_3$ (x=0.2). With increase in doping concentration the mode at ~230 cm^{-1} (A_{1g}) shifts towards lower frequencies at low temperature. Such a mode does not appear for x=0.1. The pressure induced blueshift in A_{1g} phonon mode frequency as observed from Table II could be due to a modification of the local symmetry at room temperature.

Eigenvalues of the dynamical matrix obtained from the potential expressed in Eq. (1) are the squared eigenfrequencies $\omega_j^2(\bar{q})$ of the oscillators. The band index j labels the $3r$ phonon branches of a solid with r atoms in the unit cell. The phonon band structure $\omega_j(\bar{q})$ is known as the dispersion relation, i.e., the relation between the phonon mode frequency ω_j and wave vector ($\bar{q}$). There are in all 30 vibrational degrees of freedom of atoms in the primitive cell of rhombohedral $La_{0.75}Ca_{0.25}MnO_3$ giving rise to 30 vibrational modes at the Brillouin zone center ($\bar{q}$=0), which are well distributed among the various irreducible representation of D_{3d}^6 in the fashion presented in Eq. (2). Figure 2 presents the phonon dispersion curves (PDC) of $La_{0.7}Sr_{0.3}MnO_3$ in high symmetry direction ($\overline{qqq}$) of the Brillouin zone (BZ) at four different pressures. The ambient pressure phonon dispersion curves of $La_{0.7}Sr_{0.3}MnO_3$ presented in Fig. 2 can be utilized to quantitatively explain the behavior of modes and their origin based on some conjectures drawn by using a quite crude classification.[26] Based on this classification the modes at high (500–700 cm^{-1}), intermediate (200–500 cm^{-1}), and low (below 200 cm^{-1}) frequencies can be ascribed to Mn-O bond stretching, tilting, or rotation of the octahedra and vibrations of the heavy rare earth La and Sr atoms, respectively. Figure 2 also includes the low temperature experimental data obtained from the inelastic neutron scattering (INS) experiments at ambient pressure for rhombohedral $La_{0.7}Sr_{0.3}MnO_3$.[46] It is seen from Fig. 2 that the phonon modes of the intermediate and higher frequency ranges are hardened with the application of pressure. This reflects that the frequencies of the modes related to the Mn-O bond and tilting or rotation of octahedra increase with the pressure which may be due to the increase of strain in the Mn-O bond. From Fig. 2, it is clear that a distinct gap between 200 and 350 cm^{-1} at zone center increases with the pressure.

In order to investigate the phonon properties, the understanding of phonon density of states is vital, as it requires the computation of phonon modes in the entire BZ. In addition, the phonon density of states presents an overall view of the range and extent of various phonon modes in the lattice and is expressed as

$$g(\omega) = A \int_{BZ} \sum_{i=1}^{N} \delta[\omega - \omega_j(q)] dq, \tag{3}$$

where A is the normalization constant and other forms have usual meaning. The phonon density of states can be used to compute the specific heat and Debye temperature. The calculations for the partial phonon density of states, $g_k(\omega)$ for the kth atom associated with eigenvector $\varepsilon_k(\bar{q}_j)$, where j is the mode index, can be expressed as

$$g_k(\omega) = B \sum_{unitcell} \sum_{jp} \delta[\omega - \omega_j(q_p)] |\varepsilon_k(q_p, J)|^2 dq_p, \tag{4}$$

where B is the normalization constant. The knowledge of partial phonon density of states enables us to determine the mean square displacements of various atoms, which in turn leads to the determination of the vibrational amplitudes of individual atoms. This also tells us how particular atoms move in particular directions as a function of phonon energy, which is very useful for the interpretation of the inelastic neutron scattering data.

To understand the origin of peaks in the total phonon density of states (DOS), we examine the ambient condition spectra of total DOS along with the partial DOS displayed in Fig. 3(a). From the partial and total phonon DOS some conjectures can be drawn exploiting a crude classification based on the atomic contributions. Hence, the total DOS can be classified into three regions: (1) in region below 100 cm^{-1}, peaks in DOS correspond to La/Sr, Mn, and O vibrations. (2) The region between 100 and 400 cm^{-1} is prominently due to La/Sr and O vibrations. (3) The major contribution of oxygen atoms prevails in the region after 400 cm^{-1}, which is

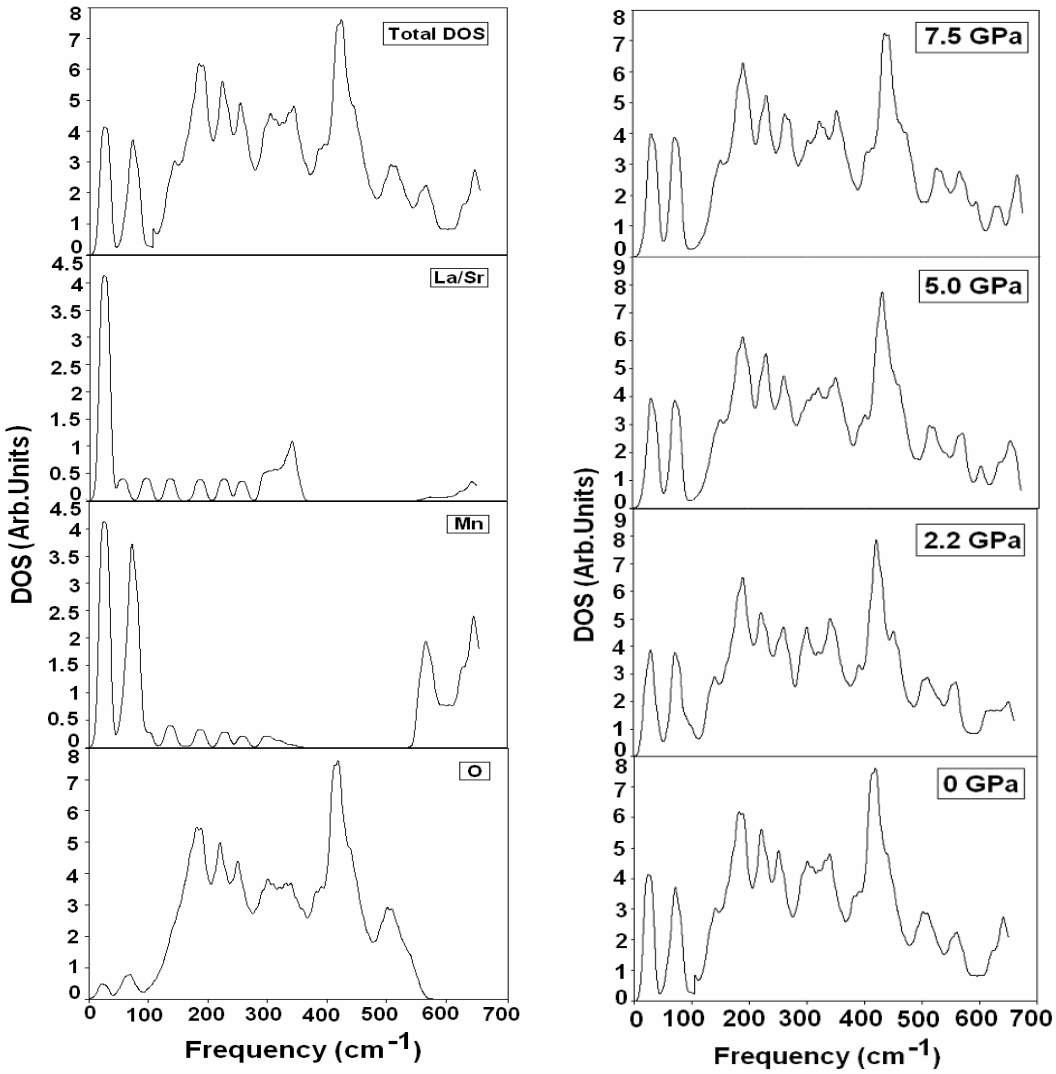

FIG. 3. (a) Total and partial one phonon density of states of $La_{0.7}Sr_{0.3}MnO_3$. (b) Pressure variation of the total phonon density of states.

mainly due to the frequencies associated to the Mn-O bond stretching. The classification based on the octahedra has already been discussed above. Figure 3(b) presents the total phonon DOS at different pressures and reveals that there is a pronounced shift in the peak positions and change in their shapes as the pressure is increased. The most prominent change observed is that the peaks after 600 cm^{-1}, 400 cm^{-1}, and 300 cm^{-1} evolve and further sharpens with the increase in pressure. The sharpening of the peaks can be attributed to the reduction of broadening of phonon peaks due to the shortage of charge introduced by the pressure, which reduces the JT distortion in MnO_6 octahedra and decreases to some extent the lattice disorder. As a matter of fact, both electron-phonon interaction and structural disorder cause an increase of phonon lifetime thus closing the peak profiles.[20,26] The shift of the peak positions in the DOS can be attributed to the variation in the percentage contribution of individual atoms with the pressure.

For a solid at a temperature T, the mean number of phonons with energy $\hbar\omega_j(\bar{q})$ is given by the Bose-Einstein distribution $n_{jq}(T)=\left[\exp\frac{[\hbar\omega(\bar{q})]}{K_BT}-1\right]^{-1}$. The mean square displacement of a single quantum mechanical harmonic oscillator, $\langle u^2\rangle=\left(\frac{\hbar}{m\omega}\right)\left(n+\frac{1}{2}\right)$ can easily be generalized to that of a single atom in the direction i as

$$\langle u_{ki}^2\rangle=\left[\frac{V}{2\pi^3}\right]\cdot\left(\frac{\hbar}{m_k}\right)\sum\int_{BZ}|\varepsilon_{jkl}(\bar{q})|^2\left[\frac{\left\{n_{jq}(T)+\frac{1}{2}\right\}}{\omega_j(\bar{q})}\right]d\bar{q}. \tag{5}$$

It can be seen from the above expression that light atoms vibrating at low frequencies exhibit large zero point motions. The off diagonal elements $\langle\bar{u}_{ki}\bar{u}_{kj}\rangle$ can be calculated in a similar way. The thermal and zero point motion of the atoms are often described using the matrix of anisotropic temperature factors $\bar{B}$. For an atom k, it is defined by

$$\bar{B}_{ij}(\bar{k})=8\pi^2\langle\bar{u}_{ki}\bar{u}_{kj}\rangle. \tag{6}$$

The pressure dependent anisotropic temperature factors $\bar{B}$ at 300 K calculated by using Eq. (6) are presented in Table III.

TABLE III. Vibrational amplitudes of individual atoms of $La_{0.7}Sr_{0.3}MnO_3$ at 0, 2.2, 5.0, and 7.5 GPa at room temperature.

	$8\pi^2\langle u^2\rangle/3$ (Å)			
Atoms	0 GPa	2.2 GPa	5.0 GPa	7.5 GPa
La/Sr	3.2680	3.2063	3.0889	3.0301
Mn	1.5516	1.5117	1.4513	1.4126
O	0.6954	0.6777	0.6542	0.6368

The lattice excitations play a key role in the discussion of two generic ground states, ferromagnetism and charge order observed in the perovskite manganites. The lattice excitation is proportional to $\exp(-2W)$, where W being the Debye-Waller factor and expressed as $2W(\vec{q})=\langle(\vec{q}\cdot\vec{u})^2\rangle$ with the atomic displacement $\langle u(T)^2\rangle$. Normally the temperature dependence of the atomic displacement is corrected with the lattice distortion via the effective Grüneisen parameter γ_{eff} for any system. Since the pressure also causes the distortion such as the temperature, pressure dependence of the atomic displacement at fixed temperature can be correlated with the lattice distortion and the effective Grüneisen parameter γ_{eff}. The effective Grüneisen parameter can be expressed as $\frac{W(P_2)}{W(P_1)}=\left[\frac{V(P_2)}{V(P_1)}\right]^{2\gamma_{eff}}$,[47] where $V(P_i)$: $i=1,2$ represents the volume at pressure P_i. It is observed that the typical value of effective Grüneisen parameter is in the range of 2–3 for most of the ordered solids.[14] In the present case, the effective Grüneisen parameter γ_{eff} has been calculated for three different regions between 0 to 7.5 GPa. The value of γ_{eff} is 2.78, 1.19, and 0.87 for 0–2.2, 2.2–5, and 5–7.5 GPa, respectively. The variation in γ_{eff} is so dramatic that its value drops rapidly from the quite high value of 2.78 in the range of 0–2.2 GPa to 0.87 in the range of 5–7.5 GPa. These values of γ_{eff} reflect that the γ_{eff} decreases for the range of pressure going from lower to higher which is in agreement with the idea of a pressure-induced reduction of the JT distortion.[1]

The pressure dependent lattice specific heat at constant volume of $La_{0.7}Sr_{0.3}MnO_3$ has been calculated by using the phonon density of states and can be expressed as

$$C_V(T)=K_B\int\left(\frac{h\omega}{2\pi K_BT}\right)^2\left[\frac{\exp\left(\frac{h\omega}{2\pi K_BT}\right)}{\left[\exp\left(\frac{h\omega}{2\pi K_BT}\right)-1\right]^2}\right]g(\omega)d\omega, \tag{7}$$

where $g(\omega)$ is the total phonon DOS. The values of room temperature specific heat at constant volume for the considered manganite are 104.6, 105.07, 104.55, and 104.1 J/mol K at 0, 2.2, 5.0, and 7.5 GPa, respectively. It can be seen that there is no significant difference between the values of C_V for all considered pressure; however, a slight increase in C_V at 2.2 GPa indicates lattice expansion under pressure which further reduces upon increase in pressure. Since the present results could not be compared with the experimental data, however, their values are reasonably close to the experimental value of C_P (125 J/mol K) for $La_{0.75}Sr_{0.25}MnO_3$ (Ref. 48) and give confidence to the present model calculation.

TABLE IV. A_{1g} and E_g phonon modes in $La_{1-x}A'_xMnO_3$ (A' = Sr, Ba, and Pb; $x=0.3$).

Modes (cm^{-1})	$La_{0.7}Sr_{0.3}MnO_3$	$La_{0.7}Ba_{0.3}MnO_3$	$La_{0.7}Pb_{0.3}MnO_3$
A_{1g}	210.78	216.08	264.10
E_g	29.08	52.15	83.80
	174.25	188.05	257.50
	408.72	464.05	449.60
	447.57	506.78	489.32

It is a known fact that the phase diagram of manganites depends very much on several variables such as pressure, applied magnetic field, doping concentration x, temperature, and A site average atomic radius ($\langle r_A\rangle$).[1–5] Temperature dependent diffraction measurements show that the JT distortion of MnO_6 octahedra in the insulating state reduces at IM transition.[49] The Mn^{+3} to Mn^{+4} ratio changes due to the effect of external parameters and results into a change in the Mn-O bond length and Mn-O-Mn bond angle and hence in the perovskite structure. Increase in $\langle r_A\rangle$ has been found responsible for the reduction of the octahedral distortion, enhancement of the metallic character and increase in T_C (Refs. 50 and 51) similar to the effect of external pressure.[1,21] Since IM transition can be related with the narrowing of octahedra and frequency hardening of the octahedral bending and stretching modes, it will be of interest to see the effect of internal pressure determined by $\langle r_A\rangle$ on the phonon modes of manganites and find if there is any correlation between the internal (chemical) and external (applied) pressure effect at least on phonons. It is expected that the increase in average atomic dimension at the A site will enhance the pressure (internal) which may reduce the free volume around the A site and finally the IM transition. In this case the octahedra become distorted and the Mn-O-Mn angle tends to 180°.[1] We therefore, extend our investigation to the phonon properties of $La_{0.7}A'_{0.3}MnO_3$ (A', Pb, and Ba) at ambient pressure not only to see the behavior of phonons in Ba and Pb doped $LaMnO_3$ in addition to Sr doped system reported above but also to see the effect of internal pressure determined by the average atomic radius, $\langle r_A\rangle$. Since the present study mainly focuses on the pressure (external) dependent phonon behavior in $La_{0.7}Sr_{0.3}MnO_3$, the detailed $\langle r_A\rangle$ dependent phonon properties are not reported here. However, an effort is made to analyze the effect of internal and external pressures on the phonon modes particularly related to the MnO_6 octahedra and phonon spectrum (DOS). Our choice for the Ba and Pb doped systems along with the Sr doped $LaMnO_3$ is due to the crystallographic structure as they all belong to the same rhombohedral structure at $x=0.3$ doping concentration. The crystallographic structure parameters of the $La_{0.7}Ba_{0.3}MnO_3$ and $La_{0.7}Pb_{0.3}MnO_3$ for the calculation of phonon properties are used from Refs. 49 and 52.

Table IV presents the A_{1g} and E_g Raman active phonon modes of $La_{0.7}Sr_{0.3}MnO_3$, $La_{0.7}Ba_{0.3}MnO_3$, and

$La_{0.7}Pb_{0.3}MnO_3$. The results for Pb and Ba doped systems could not be compared with any measured data, while the comparison for the Sr doped system is already made in Table II and discussed above. As mentioned above, A_{1g} and E_g modes are directly related with the octahedron, we restrict the discussion to these phonon modes only. Table IV reveals that the A_{1g} mode arising due to the rotation of MnO_6 octahedra shows different behavior in the present case than the one observed under external pressure. The frequency of the A_{1g} mode increases with the increase of $\langle r_A \rangle$ similar to the effect of external pressure, but a dramatic increase is observed for Pb-doped $LaMnO_3$ which has the highest $\langle r_A \rangle$ of 1.399 Å (Ref. 53) in these considered manganite systems. The average A-site atomic radii for Sr and Ba doped $LaMnO_3$ are 1.24 Å and 1.29 Å, respectively.[49] This increase of the frequency of A_{1g} mode for the Pb doped system is quite large in comparison to the external pressure even at maximum considered pressure of 7.5 GPa for Sr doped compound in the present study. The hardening of A_{1g} phonon mode with increasing internal pressure determined by $\langle r_A \rangle$ indicates that there is a reduction in the el-ph interaction and hence in the distortion of the octahedral with the increase of internal pressure similar to the external pressure. The similar trend is observed for the E_g modes except for the higher frequency modes involving oxygen atom vibration and Mn-O bond length. A remarkable feature is observed for the Pb doped $LaMnO_3$ compound that the frequency of higher E_g modes involving oxygen atom vibrations and Mn-O bond length decreases in spite of the increase of $\langle r_A \rangle$, a trend opposite to the Ba doped system. While the small increase of $\langle r_A \rangle$ i.e., going from Sr to Ba doped system shows more or less the same trend of increase of frequency similar to the effect of applied pressure, the frequencies for Pb doped system where there is a large increase in $\langle r_A \rangle$, are different. In considered manganites, a distinct increase in the frequency of A_{1g} and two E_g phonon modes and a significant decrease in the higher frequency E_g modes of Pb doped system are observed with reference to Ba doped $LaMnO_3$. Although these calculated frequencies or the trend could not be compared with any theoretical or experimental data, a conclusion can be drawn for the different trend in frequencies based on changes in octahedra of rhombohedral ($R\bar{3}c$) Sr, Ba, and Pb doped $LaMnO_3$ cause due to two different modes of pressure. An analogy can be seen from the temperature and concentration dependent Raman measurement on $La_{1-x}Sr_xMnO_3$ performed by Bjornsson *et al.*[43] which shows the appearance of a new A_{1g} Raman active phonon mode with the increase of Sr concentration from $x=0.1$ to $x=0.2$, i.e., increasing the internal pressure. The reason for the frequency of A_{1g} and two lower E_g modes closure in Sr and Ba doped and relatively significant difference for A_{1g} mode and decrease of two E_g modes frequency in Pb doped system may be correlated with the low and high $\langle r_A \rangle$. At low $\langle r_A \rangle$ both the increase of the Mn-O-Mn bond angle and the decrease of Mn-O bond length contribute to the A_{1g} and E_g modes, while at high $\langle r_A \rangle$, the two structural parameters have opposite effects.[49] This may be the reason for the increase in A_{1g} and E_g frequencies of Ba doped system and significant increase in A_{1g} and decrease in the higher frequency E_g modes of Pb doped system in comparison to the Ba doped $LaMnO_3$ compound as these modes arise due to the Mn-O-Mn bond angle and Mn-O bond length, respectively. It is also observed that A_{1g} phonon mode frequency is expected to increase both as functions of increasing $\langle r_A \rangle$ and applied pressure. However, the rate of increase of frequency for low $\langle r_A \rangle$ and applied pressure is similar and slow but for high $\langle r_A \rangle$, it is faster. The application of external pressure on these compounds produces quite different structural effects than the chemical or internal pressure. The external pressure compresses all bond lengths and a slight increase of the Mn-O-Mn bond angle while the internal pressure enhances Mn-O-Mn bond angle but suppresses Mn-O bond length. The anomalous change in the frequency of A_{1g} mode for $La_{0.7}Pb_{0.3}MnO_3$ may be due to some abrupt reduction of JT distortion and el-phonon interactions.

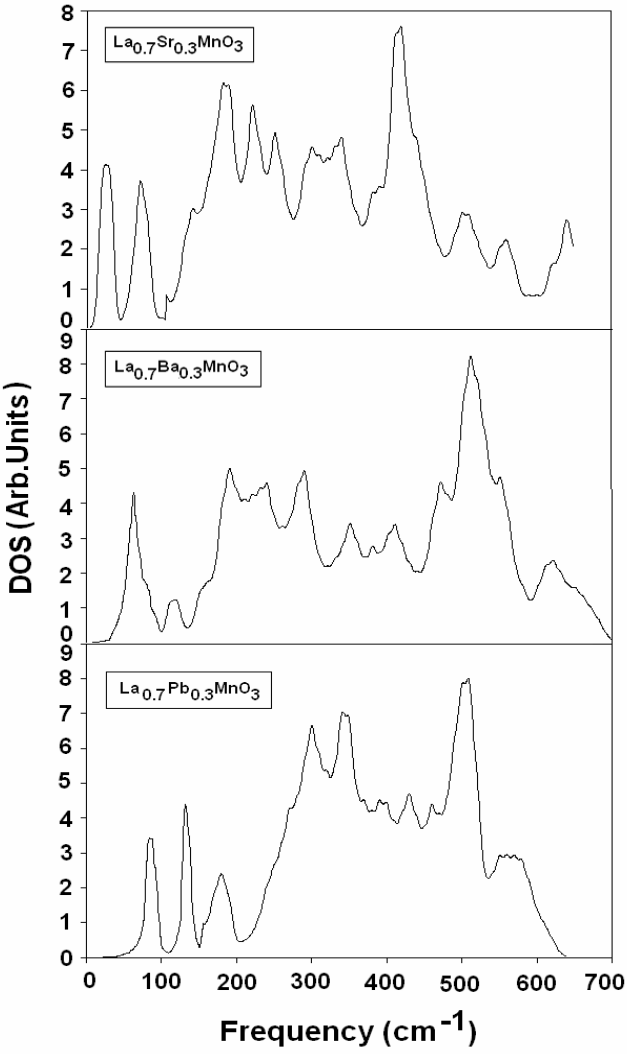

FIG. 4. Total phonon density of states of $La_{1-x}A'_xMnO_3$ (A' =Sr, Ba, and Pb; $x=0.3$).

In Fig. 4, we present the phonon density of states (phonon spectrum) of Sr, Ba, and Pb doped $LaMnO_3$ compounds for the same value of concentration (x) to see the effect of A site average atomic radius $\langle r_A \rangle$ on the phonon spectrum. Figure 4 reveals that there are prominent shifts of the peak positions

and change in their shapes on increasing $\langle r_A \rangle$. There is a gradual shift of last peak in Sr doped system to lower wave numbers going from Sr to Pb, i.e., increasing $\langle r_A \rangle$. Also the three small peaks at $\sim 500\ cm^{-1}$ in Sr doped system gets converted into two with sharpness in the case of Ba doped system and to a very sharp peak at $500\ cm^{-1}$ and one broad and small peak centered around $550\ cm^{-1}$ in the case of Pb doped system. The prominent peak at about $450\ cm^{-1}$ observed in Sr doped system almost disappears in Ba and Sr doped $LaMnO_3$. A noticeable difference in the middle region of the spectra is clearly visible. The peaks in the spectrum from 200 to 275 cm^{-1} in $La_{0.7}Sr_{0.3}MnO_3$ start diminishing in Ba doped system and finally disappear in Pb doped system. A shoulder in the case of Sr doped system evolves in a well defined peak below $200\ cm^{-1}$ in the case of Pb doped system. The two phonon peaks observed below $100\ cm^{-1}$ in La-Pb and La-Sr system convert into one very prominent and sharp peak in Ba doped system due to almost the same mass for La and Ba atoms. As far as the comparison between the phonon spectra under the influence of two different modes of pressure is concerned, it is seen from Figs. 4 and 3(b) that the effect of internal pressure determined by average *A*-site atomic radius is more prominent and spectra changes significantly.

IV. CONCLUSIONS

In conclusion, the present paper reports a theoretical lattice dynamical model calculation to investigate the phonon properties of $La_{0.7}Sr_{0.3}MnO_3$ under pressure up to 7.5 GPa. Pressure dependence of the zone center phonon modes, phonon dispersion, and phonon DOS have been obtained for rhombohedral $La_{0.7}Sr_{0.3}MnO_3$. The computed zone center phonon frequencies at ambient pressure are seen to agree fairly well with the available experimentally observed values. The A_{1g} mode is the most sensitive to pressure variation, which seems to be related with the changes in JT distortion. High frequency phonon modes, which are associated with the MnO_6 octahedra show almost linear pressure induced hardening while the low frequency phonon modes, which actually do not depend on the octahedral distortion, are almost pressure independent. The hardening of phonon modes with the increase in pressure accompanied by the dispersion in high symmetry directions are well observed in phonon dispersion curves. The shift in peak positions and changes in their shapes associated with the lattice structure modifications with increase in pressure are also observed in the total phonon density of states. The phonon peaks in the higher energy side of the phonon DOS show decrease in peak width with the increase of pressure and hence there appears reduction in electron-phonon interaction and lattice disorder responsible for the JT distortion. It is observed that the phonons in manganites are sensitive to both chemical pressure induced by average *A*-site atomic radius $\langle r_A \rangle$ and applied external pressure. Therefore, it is seen from the present study of the internal pressure determined by the average *A*-site atomic radius $\langle r_A \rangle$ and applied pressure that the effect of both pressures is to reduce the el-ph interaction. The effect of pressure which decreases the Mn-O-Mn bond length of MnO_6 octahedra results into the reduction of el-ph interaction and therefore can be correlated with the observed magnetostructural properties. The weakening of el-ph interaction reflects the metallicity of the system and therefore the hardening of phonon modes which is responsible for reducing the el-ph interaction makes the system insulator to metal through the IM transition. Substantially linear pressure dependence of A_{1g} phonon mode and comparison within the observed $\langle r_A \rangle$ dependence suggests the equivalence between internal and external pressure to hold for low $\langle r_A \rangle$ while for larger $\langle r_A \rangle$ both effects are different. Our investigation indicates that the pressure tuned el-ph interaction for low $\langle r_A \rangle$ and lower applied pressure the structural effects become more important at larger $\langle r_A \rangle$. The effective mode Grüneisen parameter depicts that the pressure induces the reduction of JT distortion, which is the signature of the rhombohedral structure.

ACKNOWLEDGMENTS

The financial assistance from the DST and DAE-BRNS, Government of India is acknowledged. One of us, M.K.T., would like to thank the Council of Scientific and Industrial Research, New Delhi for their financial support. The authors are extremely grateful to Mikhail Smirnov for making available the lattice dynamical code LADY. P.K.J. is thankful to the TWAS-UNESCO and CBPF for their financial support and local hospitality, respectively, during which part of the work is completed.

*Present address: Centro Barsileiro de Pesquisas Fisicas–CBPF, Rua Dr. Xavier Sigaud 150, Rio de Janeiro, RJ-CEP: 22290-180, Brazil.

[1] H. Y. Hwang, T. T. M. Palstra, S.-W. Cheong, and B. Batlogg, Phys. Rev. B **52**, 15046 (1995).

[2] R. M. Kusters, J. Singleton, D. A. Keen, R. McGreevy, and W. Hayes, Physica B **155**, 362 (1989).

[3] R. von Helmolt, J. Wecker, B. Holzapfel, L. Schultz, and K. Samwer, Phys. Rev. Lett. **71**, 2331 (1993).

[4] G. M. Jonker and J. H. van Santen, Physica (Utrecht) **16**, 337 (1950).

[5] A. J. Millis, Nature (London) **392**, 147 (1998); J. Fontcuberta, Phys. World **12**, 33 (1999).

[6] For a review, see *Colossal Magnetoresistance Oxides*, edited by Y. Tokura (Gordon and Breach, London, 1999).

[7] C. Zener, Phys. Rev. **82**, 403 (1951); P.-G. de Gennes, *ibid.* **118**, 141 (1960); P. W. Anderson and H. Hasegawa, *ibid.* **100**, 675 (1955).

[8] A. J. Millis, P. B. Littlewood, and B. I. Shraiman, Phys. Rev. Lett. **74**, 5144 (1995); A. J. Millis, B. I. Shraiman, and R. Mueller,

ibid. **77**, 175 (1996).
[9] M. B. Salamon and M. Jaime, Rev. Mod. Phys. **73**, 583 (2001).
[10] Y. Tokura and Y. Tomioka, J. Magn. Magn. Mater. **200**, 1 (1999).
[11] J. M. D. Coey, M. Viret, and S. von Molnar, Adv. Phys. **48**, 167 (1999).
[12] M. Imada, A. Fujimori, and Y. Tokura, Rev. Mod. Phys. **70**, 1039 (1998).
[13] T. Venkatesan, M. Rajeswari, Z.-W. Dong, S. B. Ogale, and R. Ramesh, Philos. Trans. R. Soc. London, Ser. A **356**, 1661 (1998).
[14] A. P. Ramirez, J. Phys.: Condens. Matter **9**, 8171 (1997).
[15] C. N. R. Rao and A. K. Cheetham, Adv. Mater. (Weinheim, Ger.) **9**, 1009 (1997).
[16] M. Itoh, K. Nishi, J. D. Yu, and Y. Inaguma, Phys. Rev. B **55**, 14408 (1997).
[17] Y. Moritomo, A. Asamitsu, and Y. Tokura, Phys. Rev. B **56**, 12190 (1997).
[18] V. Laukhin, B. Martinez, J. Fontcuberta, and Y. M. Mukovskii, Phys. Rev. B **63**, 214417 (2001).
[19] D. P. Kozlenko, I. N. Goncharenko, B. N. Savenko, and V. I. Voronin, J. Phys.: Condens. Matter **16**, 6755 (2004).
[20] A. Congeduti, P. Postorino, E. Caramagno, M. Nardone, A. Kumar, and D. D. Sarma, Phys. Rev. Lett. **86**, 1251 (2001).
[21] V. Laukhin, J. Fontcuberta, J. L. Garcia-Muñoz, and X. Obradors, Phys. Rev. B **56**, R10009 (1997).
[22] Y. Moritoma, A. Asamitsu, H. Kuwahara, and Y. Tokura, Nature (London) **380**, 141 (1996).
[23] V. B. Podobedov, A. Weber, D. B. Romero, J. P. Rice, and H. D. Drew, Solid State Commun. **105**, 589 (1998).
[24] J. D. Lee and B. I. Min, Phys. Rev. B **55**, 12454 (1997); U. Yu, B. I. Min, and J. D. Lee, Phys. Rev. B **61**, 84 (2000).
[25] K. H. Kim, J. Y. Gu, H. S. Choi, G. W. Park, and T. W. Noh, Phys. Rev. Lett. **77**, 1877 (1996).
[26] S. Yoon, H. L. Liu, G. Schollerer, S. L. Cooper, P. D. Han, D. A. Payne, S.-W. Cheong, and Z. Fisk, Phys. Rev. B **58**, 2795 (1998); M. V. Abrashev, V. G. Ivanov, M. N. Iliev, R. A. Chakalov, R. I. Chakalovo, and C. Thomson, Phys. Status Solidi B **215**, 631 (1999).
[27] X. Wang, Y. W. Pan, and Q. L. Cui, J. Solid State Chem. **160**, 307 (2001); X. Wang, Q. Cui, Y. Pan, G. Zou, J. Liu, and Gaoya Wuli Xuebao, *ibid.* **15**, 60 (2001).
[28] L. Pinsard-Gaudart, J. Rodríguez-Carvajal, A. Daoud-Aladine, I. Goncharenko, M. Medarde, R. I. Smith, and A. Revcolevschi, Phys. Rev. B **64**, 064426 (2001).
[29] D. Kozlenko and B. N. Savenko, J. Phys.: Condens. Matter **16**, 9031 (2004).
[30] C. Meneghini, D. Levy, S. Mobilio, M. Ortolani, M. Nuñez-Reguero, A. Kumar, and D. D. Sarma, Phys. Rev. B **65**, 012111 (2001).
[31] A. Urushibara, Y. Moritomo, T. Arima, A. Asamitsu, G. Kido, and Y. Tokura, Phys. Rev. B **51**, 14103 (1995).
[32] Y. Moritomo, A. Asamitsu, and Y. Tokura, Phys. Rev. B **51**, 16491 (1995).
[33] P. Postorino, A. Congeduti, P. Dore, A. Sacchetti, F. Gorelli, L. Ulivi, A. Kumar, and D. D. Sarma, Phys. Rev. Lett. **91**, 175501 (2003).
[34] J. J. Neumeier, M. F. Hundley, J. D. Thompson, and R. H. Heffner, Phys. Rev. B **52**, R7006 (1995).
[35] G. V. Lewis and C. R. A. Catlow, J. Phys. C **18**, 1149 (1985).
[36] T. S. Bush, J. Gale, C. R. A. Catlow, and P. D. Battle, Mater. Chem. Phys. **4**, 831 (1994).
[37] J. Gale, Philos. Mag. B **73**, 3 (1996).
[38] M. B. Smirnov and V. Yu Kazimirov, Preprint JINR E **14**, 159 (2001).
[39] P. K. Jha, A. Troper, I. C. da Cunha Lima, M. Talati, and S. P. Sanyal, Physica B **366**, 153 (2005).
[40] P. K. Jha, Phys. Rev. B **72**, 214502 (2005).
[41] E. Granado, N. O. Moreno, A. García, J. A. Sanjurjo, C. Rettori, I. Torriani, S. B. Oseroff, J. J. Neumeier, K. J. McClellan, S.-W. Cheong, and Y. Tokura, Phys. Rev. B **58**, 11435 (1998).
[42] L. Martín-Carrón, A. de Andrés, M. J. Martínez-Lope, M. T. Casais, and J. A. Alonso, Phys. Rev. B **66**, 174303 (2002).
[43] P. Björnsson, M. Rübhausen, J. Bäckström, M. Käll, S. Eriksson, J. Eriksen, and L. Börjesson, Phys. Rev. B **61**, 1193 (2000).
[44] Ch. Hartinger, F. Mayr, A. Loidl, and T. Kopp, Phys. Rev. B **71**, 184421 (2005).
[45] W. Reichardt and M. Braden, Physica B **263**, 416 (1999).
[46] G. De Marzi, H. J. Trodahl, J. Bok, A. Cantarero, and F. Sapina, Solid State Commun. **127**, 259 (2003).
[47] P. Daí, J. Zhang, H. A. Mook, S.-H. Liou, P. A. Dowben, and E. W. Plummer, Phys. Rev. B **54**, R3694 (1996).
[48] D. Kim, B. L. Zink, F. Hellman, and J. M. D. Coey, Phys. Rev. B **65**, 214424 (2002).
[49] P. G. Radaelli, G. Iannone, M. Marezio, H. Y. Hwang, S.-W. Cheong, J. D. Jorgensen, and D. N. Argyriou, Phys. Rev. B **56**, 8265 (1997).
[50] H. Y. Hwang, S.-W. Cheong, P. G. Radaelli, M. Marezio, and B. Batlogg, Phys. Rev. Lett. **75**, 914 (1995).
[51] J. Fontcuberta, V. Laukhin, and X. Obradors, Appl. Phys. Lett. **72**, 2607 (1998).
[52] J. Gutiérrez, A. Peña, J. M. Barandiarăn, J. L. Pizarro, T. Hernăndez, L. Lezama, M. Insausti, and T. Rojo, Phys. Rev. B **61**, 9028 (2000).
[53] N. Ghosh, S. Elizabeth, H. L. Bhat, U. K. Rössler, K. Nenkov, S. Rössler, K. Dörr, and K. H. Müller, Phys. Rev. B **70**, 184436 (2004).